Unravelling ammonia adsorption mechanisms of adsorbents in humid conditions

Y. Khabzina, D. Farrusseng

Unravelling ammonia adsorption mechanisms of adsorbents in humid conditions

Y. Khabzina and D. Farrusseng*

Université de Lyon 1, UMR CNRS 5256, Institut de recherches sur la catalyse et l'environnement, IRCELYON, 2 Ave Albert Einstein, Villeurbanne F-69626, France

Abstract

Air purification of ammonia, a toxic industrial chemicals (TICs), by adsorption process on Metal-Organic Framework solids is attracting high scientific and commercial interests. While active carbon based adsorbents required high level of relative humidity for achieving proper performance ammonia capture, zeolite performance degrades in presence of humidity. For MOFs, the presence of humidity has been shown to be MOF dependent, either beneficial or detrimental. It appears that the role of humidity is of key importance and that different ammonia adsorption mechanisms co-exist depending on the material's physico-chemical features. Based on a screening of various microporous adsorbents including carbons, zeolites and MOFs, we show that in the presence of humidity, the ammonia uptake

* Corresponding author. Tel.: +33 4 72 44 53 65; fax: +0-000-000-0000 .
E-mail address: david.farrusseng@ircelyon.univ-lyon1.fr

mostly follows the Henry law of ammonia solubilization in water. At the exception of Copper based MOF, the ammonia capture is mostly correlated with the amount of "condensed water" in the micropore. We also generally observe a systematic higher uptake than the Henry law which can be attributed to the effect of confinement i.e surface-condensed phase interaction.

Ammonia adsorption, screening, MOFs, water adsorption

1. Introduction

Metal-Organic Frameworks (MOFs) are new porous compounds that came to the forefront in the early 2000s. These inorganic-organic hybrid materials exhibit regular pores ranging from micro- to mesopores whose surface can be functionalized by various moieties[1][2][3]. Some MOFs have shown very distinct adsorption and storage properties that set them apart from other classic commercial adsorbents, i.e., zeolites and carbons[4][5][6]. Today, we can acknowledge two commercial applications that use a MOF as the adsorbent[7]. Ammonia belongs to the class of toxic industrial components (TICs); it is produced worldwide in an amount of 219 million tons/year[8]. At a concentration of 500 ppm for an exposure time of 30 min, it causes irreversible effects, while at a concentration of 3400 ppm, it is lethal within 60 minutes. Beyond possible ammonia tank attacks in the event of conflicts[9], ammonia is identified as one of the high-risk chemicals used in manufacturing facilities. The presence of ammonia in the air requires the use of appropriate and efficient protective equipment such as gas masks equipped with type K filter cartridges. Commercial type K cartridges typically contain impregnated activated charcoal with sulphuric or phosphoric acid or transition metals that react with NH_3[10]. Although this type of adsorbent is efficient in humid conditions, its performance usually degrades in dry conditions[11]. The mechanism of NH_3 adsorption on a

carbon-based adsorbent in humid conditions is still unclear. It has been proposed that NH_3 is dissolved in water, which then condenses in the pores of the adsorbent[11][12][13]. To the best of our knowledge, however, no scientific report yet supports this assumption. On the other hand, zeolites perform well in dry conditions but their performance is jeopardised under humid conditions[7]. In contrast, a diverse group of MOFs have shown high NH3 adsorption capacity under dry and also humid conditions, such as CuBTC[13][14][15], MOF-74[7], FeBTC[16] and Zr-based MOFs[17]. Based on adsorption simulations at the molecular scale, Snurr[18] and co-workers have suggested that the most appropriate adsorbent should be hydrophobic in order to favour NH_3 adsorption versus that of H_2O. It appears obvious that (i) the role of humidity and possible water pore filling (film formation or "condensation") in the pores of the adsorbent is of key importance and (ii) that different NH_3 adsorption mechanisms co-exist depending on the material's physico-chemical features. It is impossible, however, to get a clear picture of the performances of different classes of adsorbents because they were not measured in a consistent way, thereby preventing any quantitative comparison. Also, water adsorption is usually not reported at the same conditions for which ammonia adsorption is recorded, which does not enable consistent adsorption mechanism hypotheses to be drawn in humid conditions.

This study aims to unravel possible ammonia uptake mechanisms, especially under humid conditions. In order to obtain comprehensive, quantitative trends, ammonia adsorption and co-adsorption under humid conditions have been measured using dynamic breakthrough experiments on a diverse set of adsorbents including zeolites, carbon molecular sieves, carbon and MOFs.

2. Experimental

2.1. Materials

The adsorbents were chosen to cover a wide variety of physico-chemical features, such as composition, pore size, surface functionalisation, etc. For MOFs, metals of several natures were considered: Zr, Ni, Zn, Fe, Cu and Al. Also, MOFs with functional groups such as $-NH_2$ and -COOH were studied, while for zeolites different structures and Si/Al ratios were selected. In order to benchmark the screened adsorbents, a commercial type K adsorbent from 3M was purchased[19] and tested in the same conditions. It is composed of hard black granules of 850-1700 µm size. All materials were pressed into pellets, crushed and sieved between 425µm and 600 µm.

UiO-66 type MOFs

Thanks to their thermal, chemical and mechanical stability and also their ability to be functionalised, UiO-66 type solids have attracted considerable interest, especially for NH3 air purification[10][17][20][21][22]. UiO-66 is made with very stable inorganic bricks $[Zr_6O_4(OH)_4]$ that are ideally bonded to twelve 1,4-benzenedicarboxylic acid (BDC) ligands (each Zr atom is 8-coordinated) leading to a micropore of 6 Å and 8 Å diameter. UiO-66-fumarate has tetrahedral cavities of 5 Å in diameter and a 7 Å octahedral cavity[23]. Functionalized UiO-66 such as UiO-66-NH_2 and UiO-66-COOH are prepared with 2-aminoterephthalic acid and 1,2,4-benzenetricarboxylic acid, respectively, instead of BDC. The UiO-66-COOH was obtained following the green synthesis recipe of Reinsh[24]. UiO-66, UiO-66-NH_2, UiO-66-fumarate were prepared by spray drying following the protocol

84 described in Carné-Sànchez et al.[25] and supplied by ICN2 in the framework of the EC
85 program PRODIA.

86 **CPO-27 type MOFs**

87 Due to their penta-coordinated open metal sites, Ni-CPO-27 and Zn-CPO-27 were
88 selected for this study. CPO-27 is a 1D microporous hexagonal channel structure with
89 calibrated pores of 12 Å[26]. Ni-CPO-27 was obtained from JM[16] and Zn-CPO-27 was
90 supplied by University of St Andrews (USTAN) in the framework of the EC program
91 PRODIA.

92 **Fe-BTC**

93 The structure of Fe-BTC is composed of trimers of iron octahedra sharing a common
94 vertex μ3-O linked by benzene-1,3,5-tricarboxylate moieties, leading to two types of
95 mesoporous cages with free apertures of 25 and 29 Å, accessible through microporous
96 windows of 5.5 and 8.6 Å[27]. Fe-BTC was obtained from JM[16].

97 **Cu-BTC**

98 Cu-BTC is composed of dimeric cupric carboxylate units that are connected with benzene-
99 1,3,5-tricarboxylate to form a three-dimensional face-centred cubic crystal. The larger pores
100 correspond to a square cross-section of approximately 9 Å in diameter, while the smaller
101 pores correspond to a tetrahedral side pocket of approximately 5 Å in diameter[28]. It
102 possesses coordinatively unsaturated metal sites (CUS) which can be responsible of the
103 reactivity of Cu with NH3[29]. CuBTC was supplied by MOF Technologies.

104 **Al-MIL-101-NH_2**

105 Al-MIL-101-NH_2 possesses Al^{3+} coordinatively unsaturated metal sites (CUS), allowing
106 its use as a mild Lewis acid[30]. The solid exhibits two types of quasi-spherical mesoporous
107 cages formed by 12 pentagonal and 16 faces, respectively. The so-called medium cavities are

accessible through 12 Å pentagonal windows, while the large cavities are communicated through the same pentagonal windows and 16 Å hexagonal windows[31]. Al-MIL-101-NH2 was synthesized using the protocol described in Hartmann et al.[32].

Zeolites

Sodium-form zeolites ZSM-5, Beta and faujasites were supplied by Zeolyst International. ZSM-5, an MFI-type zeolite, is composed of a three-dimensional network pore system with straight, parallel channels intersected by zigzag channels and with 10-membered rings of oxygen atoms controlling the entrance to the channels[33]. This zeolite type has a medium pore size of approximately 5.3 Å[33]. Faujasite-type structures are constructed from sodalite cages connected by six-membered ring pores. Spherical supercages, 11.2 Å in diameter, reside between the sodalite cages and are connected by 12-MR pores of size 7.4 Å x 7.4 Å[34]. Like faujasites, Beta zeolite has a three-dimensional, interconnected 12-MR pore system; the dimensions of its largest pores are 6.6 Å x 6.7 Å[34].

Carbon molecular sieves

The Carboxen 564 and Carbosieve G 60/80 were purchased from Sigma Aldrich. These carbon molecular sieves have a pore size from 6 to 15 Å.

2.2. Experimental set-up

The study of ammonia adsorption was carried out by breakthrough measurements. A flow of 100 mL/min containing 1200 ppm ammonia in the gas phase was passed through a 0.4 cm height adsorbent packed into a 7 mm i.d. fritted glass tube (0.15 cm^3). Prior to the breakthrough experiments, the adsorbents were first evacuated at 150°C for MOFs and 250°C for zeolites, under 100 mL/min N_2, for 30 minutes. This technique provides a quantitative evaluation of the uptake capacities of ammonia in dry or humid conditions. The experimental

set-up is shown in Figure 1. Breakthrough measurements were conducted at ambient temperature, under dry and humid conditions. Humid conditions were generated by humidifying a controlled flow of N_2 to obtain a relative humidity of 40% for the stream. For measurements in humid conditions, the adsorbents were wetted by equilibration at the testing relative humidity of 40% prior to feeding the humidified ammonia stream by the same RH. Outlet flow analysis was performed online by infrared spectroscopy. The breakthrough curves were plotted as a function of time without normalisation per unit mass (x-axis) nor per initial concentration (C0) (y-axis). The adsorption capacities of ammonia and water were evaluated by integrating the resulting breakthrough curves until the concentration C(t) reached the inlet concentration (C0)[7]. The total NH3 and water capacities were calculated on the basis of adsorbent mass.

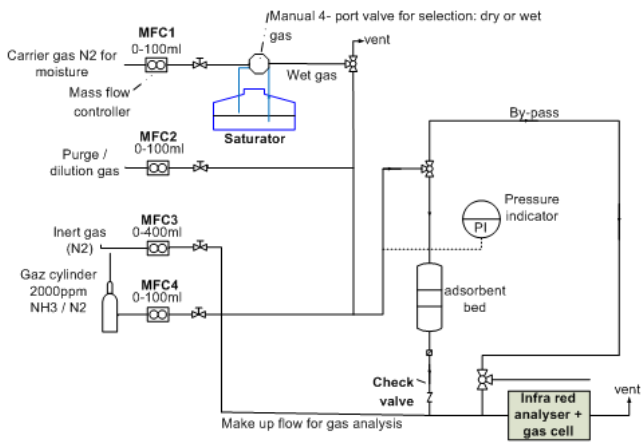

Figure 1. Experimental set-up scheme

3. Results and discussion

The breakthrough curves of the MOF adsorbents are presented here, for purposes of illustration, in Figures 2 through 5. All other breakthrough curves can be found in the SI. For

the sake of readability, the results are plotted in different figures for dry and humid conditions: UiO-type MOFs in Figures 2 and 3, and other MOFs in Figures 4 and 5.

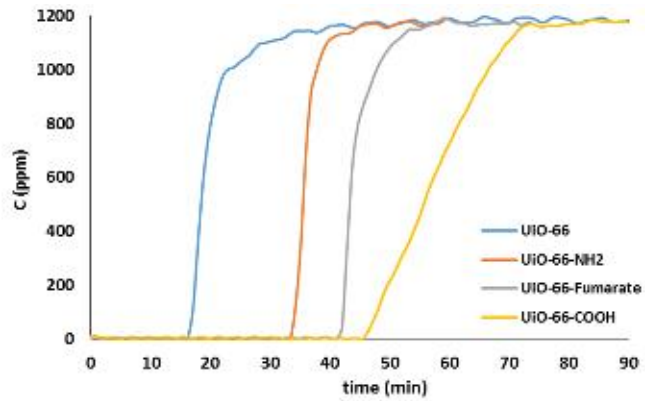

Figure 2. Ammonia breakthrough curves of UiO type MOFs in dry condition.

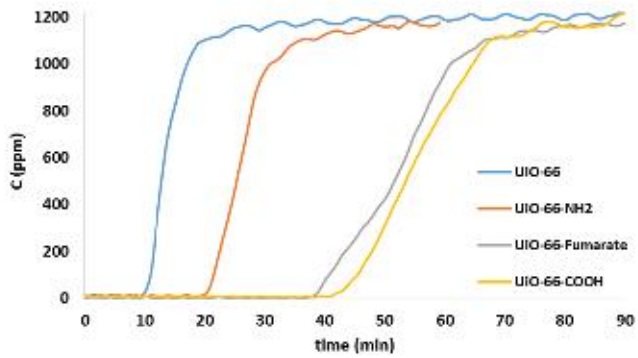

Figure 3. Ammonia breakthrough curves of UiO type MOF in humid condition.

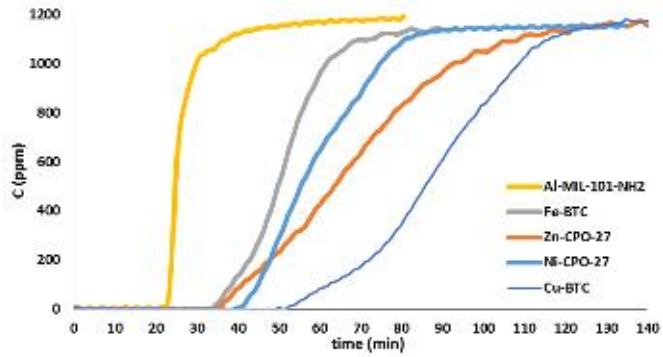

Figure 4. Ammonia breakthrough curves of various MOFs in dry condition.

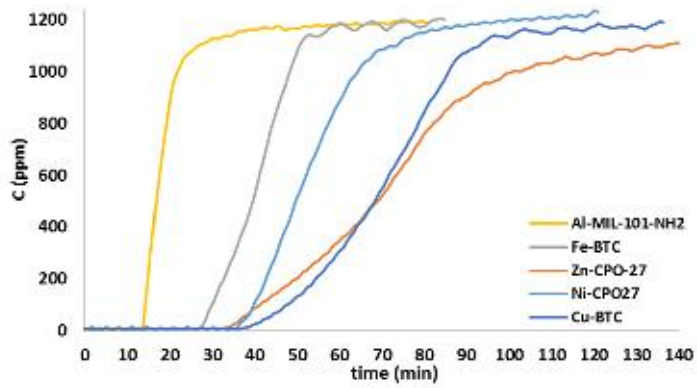

Figure 5. Ammonia breakthrough curves of various MOFs in humid condition.

Apart from different breakthrough times, we can observe different curve profiles. For some adsorbents, the concentration increases promptly after NH_3 breaks, whereas for others, the concentration increases slowly. These observations were also reported by Glover et al.[7] for a series of CPO-27. In addition, we can see that for a particular adsorbent the profiles are very similar in both dry and humid conditions, with the exception of UiO-66-fumarate. For

188 UiO-66, UiO-66-NH_2 and Al-MIL-101-NH_2, the slope is steep, whereas for others the NH3
189 concentration increases slowly until the saturation. Although we cannot rule out the effect of
190 water condensation effect under humid conditions, the rate at which the concentration
191 evolves is usually linked to the regime at which the uptake occurs, i.e., chemical or mass
192 transport controlled regimes. For steep profiles there is obviously no mass transport limitation
193 (ex. Al-MIL-101-NH_2), whereas for smooth profiles we can assume that internal mass
194 transport limitation may occur (such as for Zn-CPO-27)[21]. We can rule out different
195 packing or grain size, since all samples were sieved within a narrow fraction size range of
196 425-600 μm. The difference in breakthrough profiles may possibly arise from different grain
197 density (i.e macroporosity) after tableting, which is MOF-dependent[35]. We can assume
198 that very densely-packed crystallites may penalise the transport rate in the grains.
199
200 When comparing the NH_3 uptake data obtained here with data reported elsewhere, we can
201 observe good agreement in some cases and major apparent inconsistencies in other cases (see
202 table S1 in the SI). Regarding matching measurements, we can cite uptakes for Fe-BTC and
203 Ni-CPO-27 (40 and 58 mg/g), which are similar to those obtained by Hindocha et al.[16] (47
204 and 64 mg/g), keeping in mind that the solids were shaped and tested under slightly different
205 yet comparable conditions. We recall that the Ni-CPO-27 and Fe-BTC solids tested here were
206 supplied by Johnson Matthey[16] in the context of the "PRODIA" EC program for crossed
207 validation purposes. The sample being the same, it is not surprising to find consistent results.
208 We also see for Zn-CPO-27 very good agreement with the result obtained by Glover et al.[7]:
209 49 mg/g versus 48 mg/g. A fair matching result is also observed for Cu-BTC provided here
210 by MOFTech and that of Hindocha[16] study (112 mg/g, 105 mg/g). On the other hand, we
211 can acknowledge rather systematic inconsistencies for uptakes on UiO-66 type materials. We

note that the preparation methods used here for UiO-66 type materials are very different from methods reported elsewhere. UiO-66 and UiO-66-NH_2 were obtained by direct synthesis in a spray-dryer, whereas they were prepared using conventional batch processes in the relevant literature[17][21][20]. Also, UiO-66-COOH was prepared in water here, rather than in DMF as for Joshi et al.[22]. It is now well acknowledged that for UiO-type solids the synthesis processes and parameters have a major impact on the nature and concentration of structural defects. Lillerud et al.[36] have shown that the synthesis temperature and the use of modulators strongly modify the stability and porous structure of UiO-66 solids. It has been further shown that UiO-66 solids prepared under different conditions exhibit different water adsorption profiles38. From this literature analysis, we can conclude that although powder XRD and surface area data can be considered as fingerprints of the "quality" of the synthesis, there are insufficient for revealing the potential performances in NH_3 capture from air and conversely that the synthesis processes and parameters are key aspects, possibly as important as the selection of an ideal MOF design itself.

In our study, water breakthrough measurements at RH =40% (breakthrough curves are reported in the SI) were carried out systematically prior to NH_3 feeding; the water uptake amounts are reported in Table 1. The comparison of water uptake values with data from the literature is not straightforward, because the values reported usually correspond to 100% RH, and different values are reported for the same solids using isotherm-type measurements[6][37]. For Ni-CPO-27, Zn-CPO-27 and UiO-66-COOH, we can observe major deviations in water uptake measured by breakthrough measurements as compared to literature data. For Ni-CPO-27 and Zn-CPO-27, we found 0.31 and 0.33 g/g respectively versus 0.11 and 0.24 for Glover et al.[7] at 50% RH. In the case of UiO-66-COOH, we measured a water uptake of 0.25 g/g at 40% RH versus 0.045 g/g at 40% for Joshi et al.[22].

These discrepancies point toward differences in the surface and/or porous structural features resulting from different synthesis routes. In fact, water adsorption is a very sensitive probe for the measurement of structural defects and has recently been proposed as a characterization approach for probing the defect concentration of UiO-66 MOF[38]. Discussion about the nature of these defects is beyond the scope of this paper, and proposals can be found elsewhere38. Nevertheless, at the light of this discussion on the impact of surface defects, it is not surprising to observe different ammonia capacity data on solids which have been prepared by other methods.

We note that carbon molecular sieves are rather hydrophobic, with uptakes lower than 0.1 g/g, in contrast to the commercial carbon based adsorbent (3M) which shows a large water uptake.

The main underlying mechanism of ammonia uptake in humid conditions is revealed when the ammonia uptake is plotted as a function of the water uptake at 40% RH (c.f. Figure 6). Except for a few cases discussed below, we observe that the experimental points seem to follow a linear trend. Hence, this indicates that the ammonia uptake is determined mainly by the amount of water that is adsorbed in the adsorbent, suggesting a solubilisation-like mechanism. The solubility of NH_3 in water as a function of NH_3 pressure, assuming undissociation of NH_3, corresponds to the well-known Henry's law. We plotted the straight line corresponding to solubilized NH_3 amount as a function of the volume of adsorbed water, using a solubility of 142.8 $mgNH_3/gH_2O$ which corresponds to the Henry constant of 70 $mol.g^{-1}.bar^{-1}$ (NIST)[39] and an NH_3 pressure of 0.12 bar (corresponding to 1200 ppm). Although there are deviations, it is obvious that the linear trend very much corresponds to

Henry's law, thereby pointing to a solubilisation-like mechanism. We can propose three hypotheses that may explain the observed deviations from Henry's law. Firstly, there could be experimental errors on the amount of adsorbed water because of the high temperature sensitivity of the relative humidity. Nevertheless, we can see a general bias i.e. Henry's law underestimates most experimental data. At this stage we can question whether the Henry's law hypotheses are fulfilled. First, we shall determine whether the pores are partially or completely filled with water at 40% RH. In an earlier study, we defined the critical relative humidity value at which half of the micropore volume is filled (alpha value).

Table 1. Summarized table of ammonia and water adsorption capacities.

Adsorbent	**BET surface area (m^2/g)**	**Ammonia adsorption amount at 1200 ppm (mg/g)**		**Water adsorption amount at 0.4 RH (g/g)**	**Alpha value**
		Dry	**Wet**		
UiO-66	1120	23	26	0.11	0.30[40]
UiO66-NH_2	625	24	33	0.21	0.15[40]
UiO66-fumarate	512	42	32	0.28	0.10[23]
UiO66-COOH	614	54	54	0.25	0.2#
Ni-CPO-27	855	55	58	0.31	0.02[23]
Zn-CPO-27	373	47	49	0.33	<0.15[7]
Fe-BTC	1176	34	40	0.24	0.38[41]
Cu-BTC	1541	91	112	0.29	0.10[42]
Al-MIL-101-NH_2	3000	29	39	0.18	0.35[43]
ZSM-5 (Si/Al : 23)	384	38	25	0.13	n.d
Y (Si/Al : 14.3)	696	7	7	0.02	n.d
Y (Si/Al : 5.5)	710	31	12	0.16	n.d
Beta	549	24	24	0.14	n.d
Carboxen 564	400	0.79	2	0.02	0.70[44]
Carbosieve G	1160	10	13	0.09	>0.8[44]
Type K Adsorbent	810	39	56	0.36	n.d.

this study

For MOFs that exhibit a Type V isotherm profile (S-shape) it corresponds approximately to the inflection point of the isotherm. Except for the carbon molecular sieve, we can note that in our case, applied relative humidity of $p/p°=0.4$ is higher than the alpha value of the adsorbents, meaning that at least 50% of the micropore volume of the tested adsorbents is filled by water. On another note Henry's law supposes that the water is a bulk macroscopic phase. The physical properties of "water" in micropore shall be addressed. Indeed the arrangement of water molecules should be more similar to a multilayer of water molecules on the surface of an adsorbent, thus departing from a pure water phase. In the recent literature on zeolites, mesoporous silicates and MOFs, Ho et al.[45] have reported similar over solubility effects of gases when the "liquids" are confined in nanoporous materials. According to this study, the higher solubility of gases observed can arise either from an increased solubility due to a layering effect of the "liquid" phase or from higher adsorption at the solid-"liquid" interface. Although uptake mostly follow the Henry law, we propose that the solid surface play a major role in the adsorption mechanisms. The elucidation of molecular interactions at the surface of the different solids is beyond the scope of this study.

We wish to point out that the assumption of the solubilisation-like mechanism holds not only for the adsorbents tested in this study but also for series of UiO-66 and CPO-27 adsorbents tested elsewhere (see Figure 6, blue and purple dots)[22][7]. As we underlined above, physical properties of MOFs, especially the UiO-66 type, can depend on synthesis processes and parameters. Despite the nature and concentration of defects, we can see that the solubility mechanism assumption remains valid. As a consequence, it is possible to estimate the ammonia adsorption capacity from water uptake data regardless the nature of the porous adsorbents and their synthesis method.

We note, however, that two cases strongly depart from Henry's law. Obviously, NH3 uptakes on CuBTC and UiO-66-$(COOCu)_2$ outweigh the solubility hypothesis. For CuBTC, as cited in Peterson et al. paper[14], NH_3 reacts with the solid to produce Cu hydroxide and $(NH_4)_3$BTC species which is accompanied with the collapse of the microporous structure. From Peterson conclusions on the reactivity of CuBTC with ammonia, we can suppose here the reaction of 2 ammonia per BTC. Hence we can propose that for CuBTC, chemisorption (or reactivity) occurs in humid conditions instead of physisorption. The mechanisms of interactions between CuBTC and NH_3 in dry and humid conditions have been studied in details and can be found elsewhere[14][29].

For data on UiO-66-$(COOCu)_2$[22], we find a 1.1 relation for NH3:Cu assuming an ideal composition of the adsorbent which points toward a chemisorption/reactivity mechanism. Although the adsorption capacities of the Cu-containing MOF are well above other adsorbents tested here, their assessment for a commercial solution is out of scope of this study since there are numbers of other criteria to be fulfilled[16].

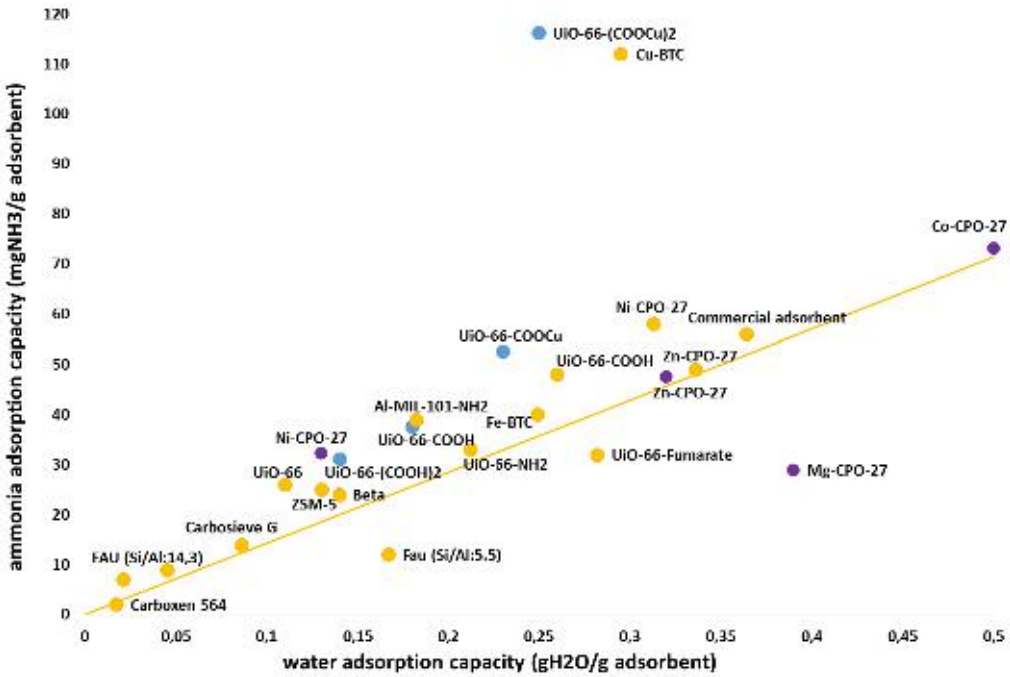

Figure 6. Ammonia uptake as a function of water uptake measured by breakthrough experiments at 40% RH and 20°C for a NH3 challenge concentration of 1200 ppm (yellow). Additional data from the literature are added: Glover et al.[7] (purple, 1294 ppm NH3) and Joshi et al.[22] (blue, 1431 ppm NH3). The straight line corresponds to the amount of NH3 solubilized in water according to Henry's law with k°H = 70 mol/kg/bar at 25°C (NIST).

In a recent study, Moghadam et al.[46] conclude from a large hypothetical screening of MOF structures that theoretical simulations show that strongly hydrophilic MOFs present highly competitive water adsorption and therefore exhibit poor selectivity towards NH_3. This conclusion goes against the experimental facts presented here. Indeed, we have clearly established, based on the screening of a diverse adsorbent library that a linear trend is observed between water uptake and ammonia uptake. While the study of solid-gas

interactions remains relevant, the bias of the study of Moghadam et al.[46] likely arises from the assumption that water is not present in "condensed" states for the NH_3 uptake simulation.

4. Conclusion

Generally speaking, the uptake mechanisms of ammonia in microporous solids for air purification can be classified in three main groups that may co-exist: (i) solubilisation, (ii) physisorption and (iii) chemisorption. We show that ammonia uptake mainly follow the Henry law suggesting a solubilisation-like mechanism which occurs when water condenses in the pore, i.e., at larger RH than the alpha value. We underline the effect of surface interactions (i.e confinement) which might be responsible for the higher uptake when comparing to the Henry law in water bulk phase. On practical aspects, it becomes possible to estimate the ammonia adsorption capacity from water uptake data regardless the nature of microporous solids or its synthesis method.

For adsorbents that are made or impregnated with reactive species such as Cu^{2+} species, chemisorption occurs to yield complexes or basic-acid adducts in a ratio close to 1:1. In addition to high uptake in the case of Cu^{2+} complexes, this mechanism offers stronger ammonia fixation, which can be an asset for K type protection filter.

Acknowledgements

This work has been carried out within the ProDIA project that has received funding from the European Union's Horizon 2020 research and innovation program under grant agreement No. 685727. The authors would like to thank Johnson Matthey, University of St

Andrews, MOF Technologies and the Catalan Institute of Nanoscience and Nanotechnology for supplying samples.

References

[1] D. Farrusseng, Metal-Organic Frameworks : Applications from Catalysis to Gas Storage, Wiley-VCH, 2011.

[2] S. Kaskel, The Chemistry of Metal-Organic Frameworks : Synthesis, Characterization, and Applications., Wiley, 2016.

[3] H. Deng, C.J. Doonan, H. Furukawa, R.B. Ferreira, J. Towne, C.B. Knobler, B. Wang, O.M. Yaghi, Science 327 (2010) 846–850.

[4] J.A. Mason, M. Veenstra, J.R. Long, H.-C. Zhou, H. Leclerc, A. Ghoufi, P. Bazin, A. Vimont, M. Daturi, T. Devic, C. Serre, G.D. Weireld, G. Maurin, Y. Han, Z. Shi, S. Feng, J. Li, Chem. Sci. 5 (2014) 32–51.

[5] H.-C. Zhou, Y. Liu, Z.U. Wang, Greenh. Gas Sci Technol 2 (2012) 239–259.

[6] M.F. de Lange, K.J.F.M. Verouden, T.J.H. Vlugt, J. Gascon, F. Kapteijn, Chem. Rev. 115 (2015) 12205–12250.

[7] T. Grant Glover, G.W. Peterson, B.J. Schindler, D. Britt, O. Yaghi, Chem. Eng. Sci. 66 (2011) 163–170.

[8] http://www.societechimiquedefrance.fr/extras/Donnees/mine/nh3/texnh3.htm.

[9] T.W. Karasik, Toxic Warfare, Santa Monica, 2002.

[10] K.-D.Henning, S.Schäfer, Gas Sep. Purif. 7 (1993) 235–240.

[11] P. Lodewyckx, Interface Sci. Technol. 7 (2006) 475–528.

[12] M. Gonçalves, L. Sánchez-García, E. de Oliveira Jardim, J. Silvestre-Albero, F. Rodríguez-Reinoso, Environ. Sci. Technol. 45 (2011) 10605–10610.

[13] C. Petit, B. Mendoza, T.J. Bandosz, Langmuir 26 (2010) 15302–15309.

[14] G.W. Peterson, G.W. Wagner, A. Balboa, J. Mahle, T. Sewell, C.J. Karwacki, J. Phys. Chem. C 113 (2009) 13906–13917.

[15] T. Watanabe, D.S. Sholl, J. Chem. Phys. 133 (2010) 94509.

[16] S. Hindocha, S. Poulston, Faraday Discuss. 201 (2017) 113–125.

[17] H. Jasuja, G.W. Peterson, J.B. Decoste, M.A. Browe, K.S. Walton, Chem. Eng. Sci. 124 (2015) 118–124.

[18] K.C. Kim, D. Yu, R.Q. Snurr, Langmuir 29 (2013) 1446–1456.

[19] https://www.amazon.co.uk/3M-A26118-6054-K1-Filter/dp/B000U6Y1P4.

[20] W.P. Mounfield, M. Taborga Claure, P.K. Agrawal, C.W. Jones, K.S. Walton, Ind. Eng. Chem. Res. 55 (2016) 6492–6500.

[21] G.W. Peterson, J.B. DeCoste, F. Fatollahi-Fard, D.K. Britt, Ind. Eng. Chem. Res. 53 (2014) 701–707.

[22] J.N. Joshi, E.Y. Garcia-Gutierrez, C.M. Moran, J.I. Deneff, K.S. Walton, J. Phys. Chem. C 121 (2017) 3310–3319.

[23] H. Furukawa, F. Gándara, Y.-B. Zhang, J. Jiang, W.L. Queen, M.R. Hudson, O.M. Yaghi, J. Am. Chem. Soc. 136 (2014) 4369–4381.

[24] H. Reinsch, Eur. J. Inorg. Chem. 2016 (2016) 4290–4299.

[25] A. Carné-Sánchez, I. Imaz, M. Cano-Sarabia, D. Maspoch, Nat. Chem. 5 (2013) 203–11.

[26] S. Cadot, L. Veyre, D. Luneau, D. Farrusseng, E. Alessandra Quadrelli, J. Mater. Chem. A 2 (2014) 17757–17763.

[27] A. Dhakshinamoorthy, M. Alvaro, H. Garcia, Adv. Synth. Catal. 352 (2010) 711–717.

[28] H. Yang, S. Orefuwa, A. Goudy, Microporous Mesoporous Mater. 143 (2011) 37–45.

[29] N. Nijem, K. Fürsich, H. Bluhm, S.R. Leone, M.K. Gilles, J. Phys. Chem. C 119 (2015) 24781–24788.

[30] A. Henschel, K. Gedrich, R. Kraehnert, S. Kaskel, Chem. Commun. (2008) 4192–4194.

[31] P. Serra-Crespo, E. V Ramos-Fernandez, J. Gascon, F. Kapteijn, Chem. Mater. 23 (2011) 2565–2572.

[32] M. Hartmann, M. Fischer, Microporous Mesoporous Mater. 164 (2012) 38–43.

[33] E. Beerdsen, D. Dubbeldam, B. Smit, T.J.H. Vlugt, S. Calero, J. Phys. Chem. B 107 (2003) 12088–12096.

[34] J.E. Krohn, M. Tsapatsis, Langmuir 22 (2006) 9350–9356.

[35] J. Dhainaut, C. Avci-Camur, J. Troyano, A. Legrand, J. Canivet, I. Imaz, D. Maspoch, H. Reinsch, D. Farrusseng, CrystEngComm 19 (2017) 4211–4218.

[36] G.C. Shearer, S. Chavan, J. Ethiraj, J.G. Vitillo, S. Svelle, U. Olsbye, C. Lamberti, S. Bordiga, K.P. Lillerud, Chem. Mater. 26 (2014) 4068–4071.

[37] J. Canivet, A. Fateeva, Y. Guo, B. Coasne, D. Farrusseng, H. Na, C. Liu, F. Sun, G. Zhu, H. Tokoro, S. -i. Ohkoshi, M. Verdaguer, A. Cabeza, C. Riekel, G. Ferey, C. Serre, Chem. Soc. Rev. 43 (2014) 5594–5617.

[38] S. Dissegna, R. Hardian, K. Epp, G. Kieslich, M.-V. Coulet, P. Llewellyn, R.A. Fischer, 19 (2017) 4035–4228.

[39] T.K. Sherwood, Ind. Eng. Chem. 17 (1925) 745–747.

[40] J. Canivet, J. Bonnefoy, C. Daniel, A. Legrand, B. Coasne, D. Farrusseng, R.Q. Snurr, G. Ferey, F. Kapteijn, M. Latroche, New J. Chem. 38 (2014) 3102–3111.

[41] Y.-K. Seo, J.W. Yoon, J.S. Lee, Y.K. Hwang, C.-H. Jun, J.-S. Chang, S. Wuttke, P. Bazin, A. Vimont, M. Daturi, S. Bourrelly, P.L. Llewellyn, P. Horcajada, C. Serre, G. Férey, Adv. Mater. 24 (2012) 806–810.

[42] Y. Cai, Y. Zhang, Y. Huang, S.R. Marder, K.S. Walton, Cryst. Growth Des. 12 (2012) 3709–3713.

[43] T. Wittmann, R. Siegel, N. Reimer, W. Milius, N. Stock, J. Senker, Chem. - A Eur. J. 21 (2015) 314–323.

[44] V. Detlev, Helmig Lee, Anal. Chem. 67 (1995) 4380–4386.

[45] L.N. Ho, Y. Schuurman, D. Farrusseng, B. Coasne, J. Phys. Chem. C 119 (2015) 21547–21554.

[46] P.Z. Moghadam, D. Fairen-Jimenez, R.Q. Snurr, M.A. Browe, K.S. Walton, Z.R. Herm, T.-H. Bae, J.R. Long, M. Lanuza, D.B. Galloway, J.J. Low, R.R. Willis, R.Q. Snurr, J.F. Stoddart, N. Planas, K. Lee, T. Pascal, L.F. Wan, D. Prendergast, J.B. Neaton, B. Smit, J.B. Kortright, L. Gagliardi, S. Bordiga, J.A. Reimer, J.R. Long, J. Mater. Chem. A 4 (2016) 529–536.